Report on

Magnus Effect: Rotating Cylinder in a Turbulent Flow

Case Study Project

Under the guidance of
Prof. Shivasubramanian Gopalakrishnan

Submitted by
Ashley Melvin

ACKNOWLEDGEMENT

I would like to express my sincere thanks to **Prof. Shivasubramanian Gopalakrishnan** for his supervision, valued suggestions and timely advices. I am extremely grateful for his patient efforts in making me understand the required concepts and principles behind this work. I would also like to thank all my friends and my parents for their continued support and encouragement, without which the report could not have been completed. I would also like to thank each and everyone who have knowingly or unknowingly helped me in completing this work.

Contents

1. Introduction

Consider an incompressible, inviscid flow over a cylinder. Theoretical analysis shows that the flow wraps around the cylinder with the flow being symmetrical in both halves of the cylinder. It has two stagnation points, one in the front and the other behind the cylinder. Such a flow is shown in fig. 1. This kind of flow leads to the theoretical result that the pressure drag is zero. In reality, that isn't the case. This is called the d'Alembert's paradox.
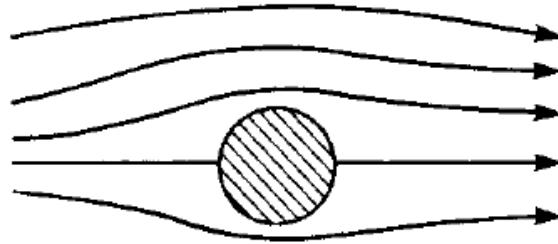
Figure 1. Ideal flow across a cylinder [1].

Now, consider the cylinder to be rotating, say in the clockwise direction. The flow field is shown in fig. 2.
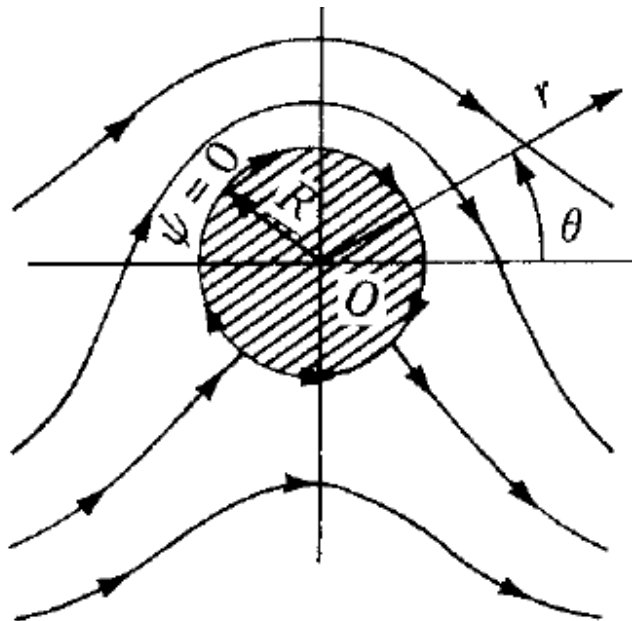
Figure 2. Flow across a rotating cylinder [1].

Above the cylinder, the flow is faster as the rotation of the cylinder is in the same direction as the free stream. Below the cylinder, the flow is slowed down as the rotation of the cylinder opposes the motion of free stream. This anomaly in flow above and below the cylinder creates a high pressure region below the cylinder and a low pressure region above the cylinder. The difference in pressure generates a lift on the cylinder.

2. Governing Equations

The Navier-Stokes equations for a viscous incompressible flow in an arbitrary domain is

$$\rho\left(\frac{\partial \vec{u}}{\partial t} + \nabla.(\vec{u}\vec{u})\right) = \nabla p + \nabla.\bar{\bar{R}} + \vec{S}_u$$

where all symbols have their usual meaning. $\bar{\bar{R}}$ is the stress tensor (symmetric) and $\vec{S}_u$ is the momentum source. The stress tensor is given by

$$\bar{\bar{R}} = \mu(\nabla\vec{u} + \nabla\vec{u}^T)$$

The Navier-Stokes equation is supplemented with the incompressibility condition

$$\nabla.\vec{u} = 0$$

Given a fluid (ρ, μ), we have four equations and four unknowns ($\vec{u}$ and p).

2.1. Lifting Flow over a Cylinder

Consider a flow that is the combination of a non-lifting flow over a cylinder and a vortex of strength Γ, as shown in fig. 3.
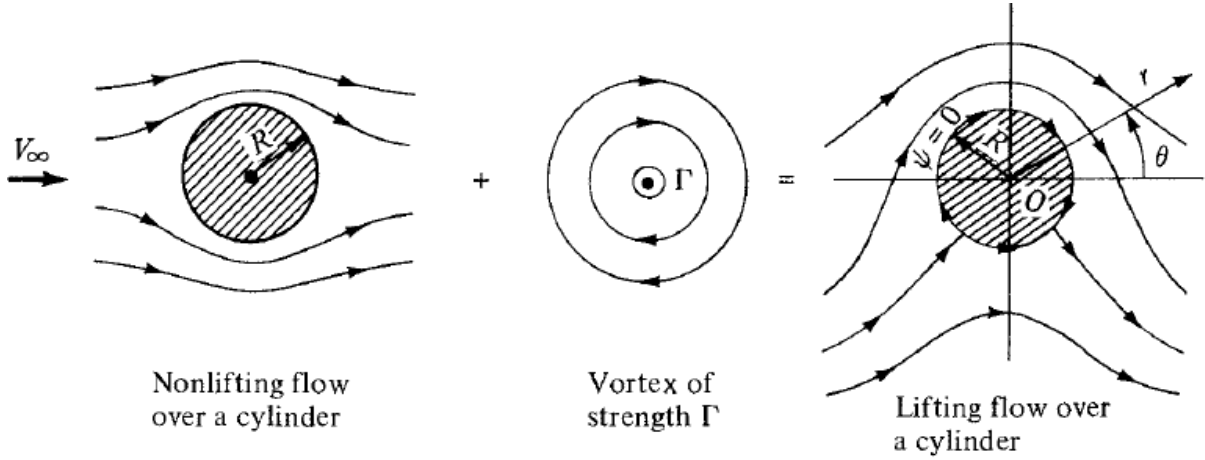

Figure 3. The synthesis of lifting flow over a cylinder [1].

The stream function for the non-lifting flow over the cylinder of radius R, in polar coordinates, is given by

$$\psi_1 = V_\infty r \sin\theta \left(1 - \frac{R^2}{r^2}\right) \tag{1}$$

The stream function for the vortex of strength Γ is given by Eq. (2). The stream function is determined by an arbitrary constant.

$$\psi_2 = \frac{\Gamma}{2\pi}\ln r + \text{const} \tag{2}$$

Since the value of the constant is arbitrary, let

$$\text{const} = -\frac{\Gamma}{2\pi}R \tag{3}$$

Combining Eq. (2) and (3),

$$\psi_2 = \frac{\Gamma}{2\pi}\ln\frac{r}{R} \tag{4}$$

The resulting stream function for the flow over a rotating cylinder is given by,

$$\psi = \psi_1 + \psi_2 = V_\infty r \sin\theta\left(1 - \frac{R^2}{r^2}\right) + \frac{\Gamma}{2\pi}\ln\frac{r}{R} \tag{5}$$

The streamlines given by Eq. (5) are sketched at the right of fig. 3.

The velocity components for the flow is given by,

$$V_r = \frac{1}{r}\frac{\partial\psi}{\partial\theta} = V_\infty \cos\theta\left(1 - \frac{R^2}{r^2}\right) \tag{6}$$

$$V_\theta = -\frac{\partial\psi}{\partial r} = -V_\infty \sin\theta\left(1 + \frac{R^2}{r^2}\right) - \frac{\Gamma}{2\pi r} \tag{7}$$

On the surface of the cylinder, $r = R$. Substituting in Eq. (6) and (7),

$$V_r = 0, \quad and \quad V_\theta = -2V_\infty \sin\theta - \frac{\Gamma}{2\pi R} \tag{8}$$

The pressure coefficient is obtained by,

$$C_p = 1 - \left(\frac{V}{V_\infty}\right)^2 = 1 - \left(\frac{V_\theta}{V_\infty}\right)^2 = 1 - \left(-2\sin\theta - \frac{\Gamma}{2\pi R V_\infty}\right)^2 \tag{9}$$

The flow is assumed to be inviscid, i.e. $c_f = 0$. Therefore, the lift coefficient on the cylinder is evaluated as

$$c_l = \frac{1}{c}\int_0^c C_{p,l}\,dx - \frac{1}{c}\int_0^c C_{p,u}\,dx \tag{10}$$

Converting to polar coordinates,

$$x = R\cos\theta \quad dx = -R\sin\theta\,d\theta$$

Therefore, Eq. (10) becomes,

$$c_l = -\frac{1}{2}\int_\pi^{2\pi} C_{p,l}\,\sin\theta\,d\theta + \frac{1}{2}\int_\pi^0 C_{p,u}\,\sin\theta\,d\theta \tag{11}$$

3

The expression for $C_{p,l}$ and $C_{p,u}$ is given by the same expression for C_p, Eq. (9). Therefore, Eq. (11) becomes,

$$c_l = -\frac{1}{2}\int_0^{2\pi} C_p \, \sin\theta \, d\theta \tag{12}$$

Substituting Eq. (9) in (12), and integrating,

$$c_l = \frac{\Gamma}{RV_\infty} \tag{13}$$

By definition, the lift per unit span is given by,

$$L' = \frac{1}{2}\rho_\infty V_\infty^2 S c_l$$

where the planform area $S = 2R(1)$. Therefore,

$$L' = \rho_\infty V_\infty \Gamma \tag{14}$$

Eq. (14) is the mathematical formulation of the Kutta-Joukowski theorem, which states that 'lift per unit span is directly proportional to circulation'.

2.2. Magnus Effect

The general ideas discussed above concerning the generation of lift on a spinning circular cylinder in a wind tunnel also apply to a spinning sphere. This explains why a baseball pitcher can throw a curve and how a golfer can hit a hook or slice - all of which are due to non-symmetric flows about the spinning bodies, and hence the generation of an aerodynamic force perpendicular to the body's angular velocity vector as shown in fig. 4. This phenomenon is called Magnus effect, named after the German physicist Gustav Magnus, who was the first person to venture on a rigorous investigation into the physics entailed.
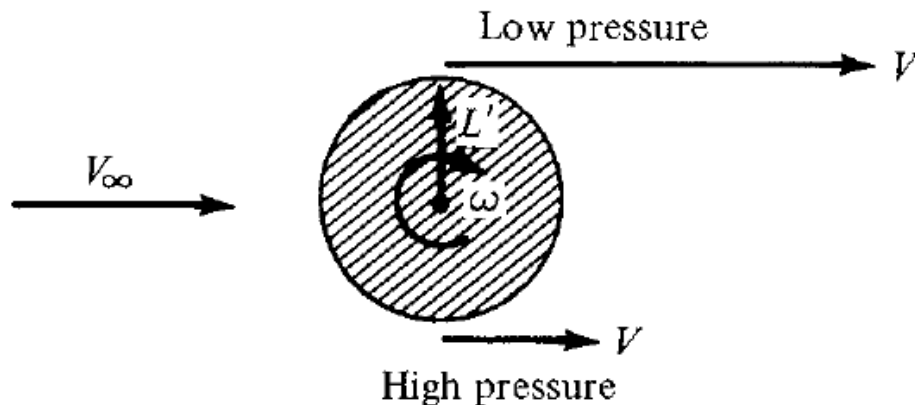

Figure 4. Generation of lift on a spinning cylinder [1].

Today, the Magnus effect has an important influence on the performance of spinning missiles; indeed, a certain amount of modern high-speed aerodynamic research has focused on the Magnus forces on spinning bodies for missile applications.

3. Implementation in OpenFOAM

3.1. Problem Statement

The problem considers unsteady, incompressible, viscous flow over a cylinder of diameter 20 cm rotating at 200 rad/s in the clockwise direction. The cross-flow is $Re = 2,00,000$, hence turbulent. The kinematic viscosity of the fluid is $\nu = 10^{-5}$ m^2/s.

3.2. Geometry & Meshing

The computational domain is shown in fig. 5. The domain is a circle of radius 2 m. The circular hole in the domain, of diameter 20 cm, is the location of the cylinder. The geometry is a disk of thickness 10 cm.
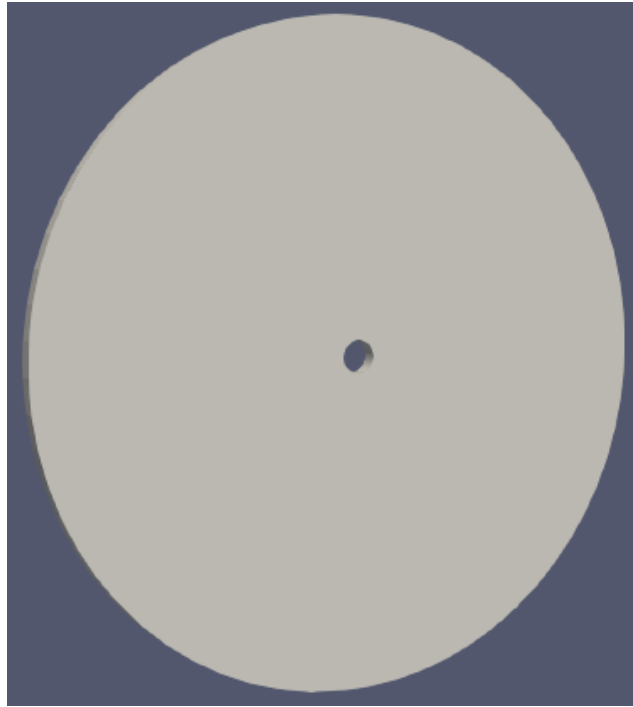

Figure 5. The configuration of flow across a rotating cylinder.

The meshing is done using Gmsh 3.0.0. Unstructured mesh is used in most of the domain except near the surface of the cylinder, where structured, refined mesh is used. The mesh in the domain and near the cylinder is shown in fig. $6a$ and $6b$.

The unstructured mesh in the domain is coarse at the domain boundary and gets finer closer to the cylinder as indicated in fig. $6a$.

The structured mesh has the same refinement throughout the section near the cylinder.

Only one cell is considered alone the z direction making the simulation 2D in xy-plane.

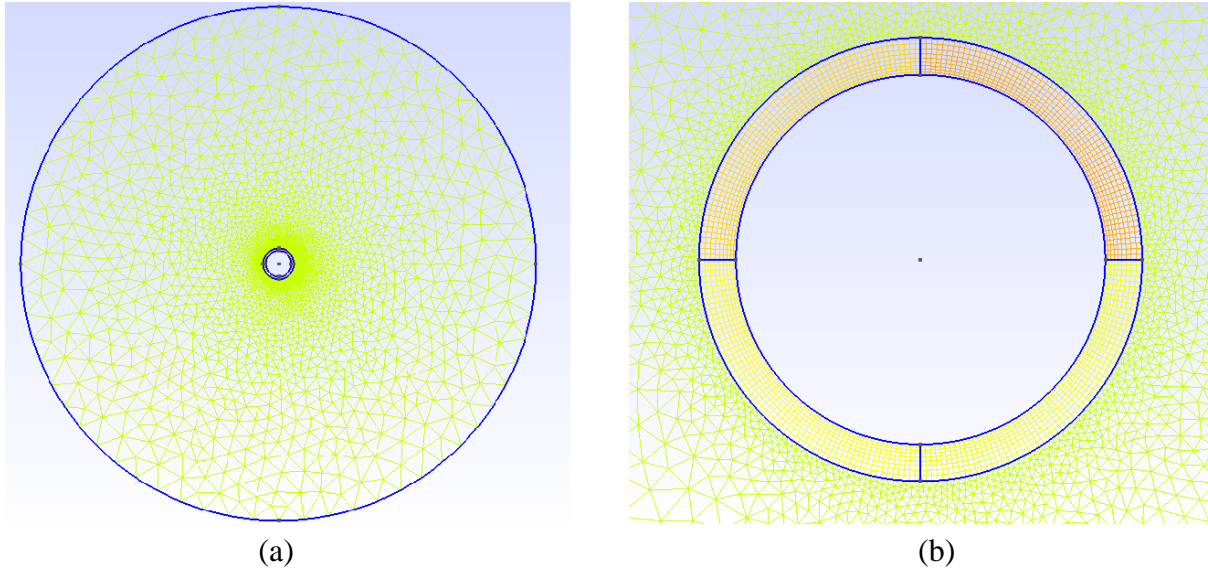(a)   (b)

Figure 6. Mesh configuration; (a) in the domain; (b) near the cylinder

3.3. Initial & Boundary Conditions

The boundary conditions for various faces are described below:

a) Domain Boundary: Outer face of the domain

Pressure (p)	Zero Gradient
Velocity vector ($\vec{u}$)	$(10, 0, 0)$ m/s

b) Cylinder: Inner face of the domain

Pressure (p)	Zero Gradient

The velocity boundary condition looks like

```
cylinder
{
    type              rotatingWallVelocity;
    origin            ( 0 0 0 );
    axis              ( 0 0 1 );
    omega             -200;
}
```

The condition says that the velocity at the cylinder boundary is rotational about the z-axis, passing through the origin and of magnitude 200 rad/s.

3.4. Solver

The turbulent flow over a rotating cylinder governing equations, as described in section 2, are solved using pimpleFoam. For turbulence modelling, the k-Epsilon RAS model is used. The value of $k = 0.00325$ and $\varepsilon = 0.000765$ are used to start the calculations throughout the domain. Respective wall functions are used on the cylinder boundary.

4. Results

The simulations are run on OpenFOAM 2.3 and the post processing is done using ParaView.

The velocity magnitude and pressure contours at $T = 1$ are shown in fig. $7a$ and $7b$ respectively.
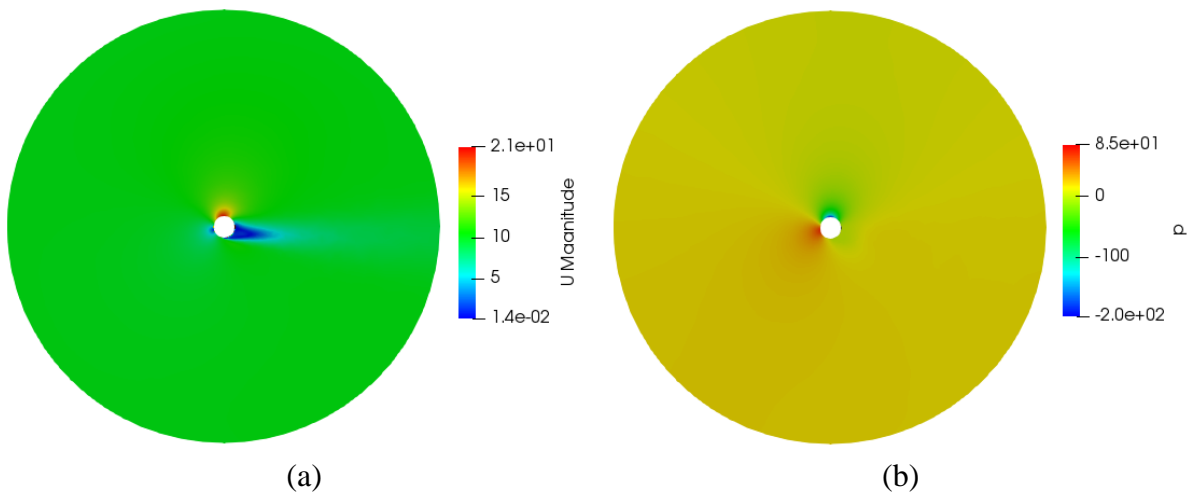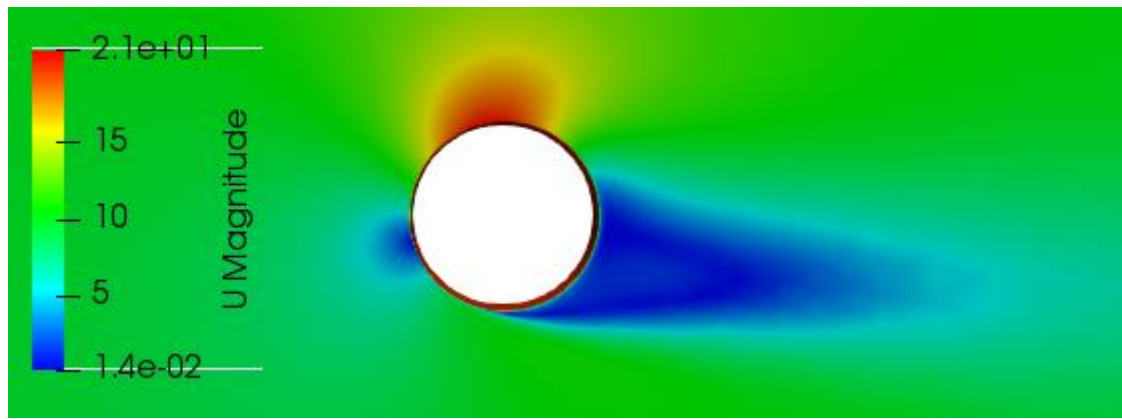

(a)   (b)

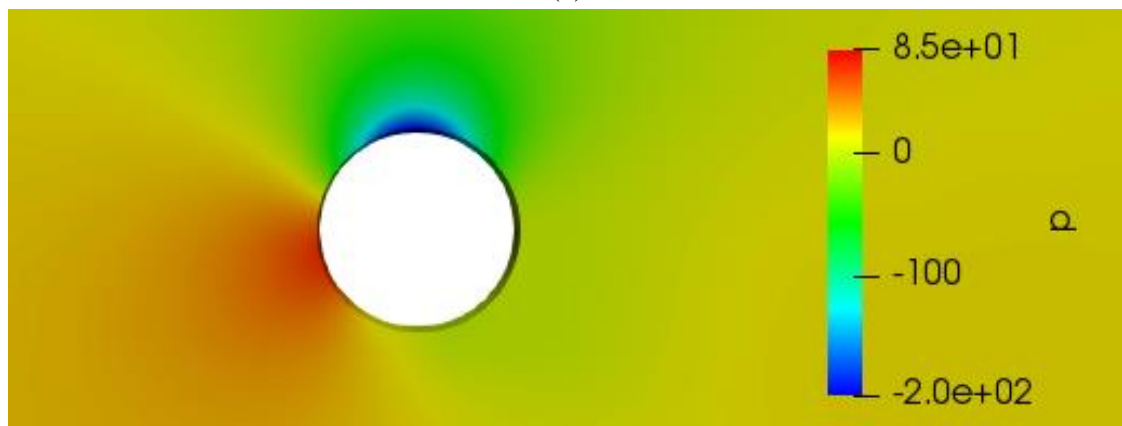Figure 7. (a) Velocity magnitude; (b) pressure contour at $T = 1$.

The velocity magnitude and pressure contours at $T = 1$ near the cylinder is shown in fig. $8a$ and $8b$.

As clearly indicated in the fig. $8a$, the flow is faster above the cylinder and slower below it. Also, the presence of 2 stagnations regions, in front and behind the cylinder, are clearly visible in fig. $8a$.

Fig. $8b$ shows that the pressure above the cylinder is less than the free stream pressure and the pressure above the cylinder is more than the free stream pressure. This disparity of pressure above and below the cylinder indicates the presence of an upward force on the cylinder, the Magnus force.

(a)

(b)

Figure 8. (a) Velocity magnitude; (b) pressure contour at $T = 1$ near the cylinder.

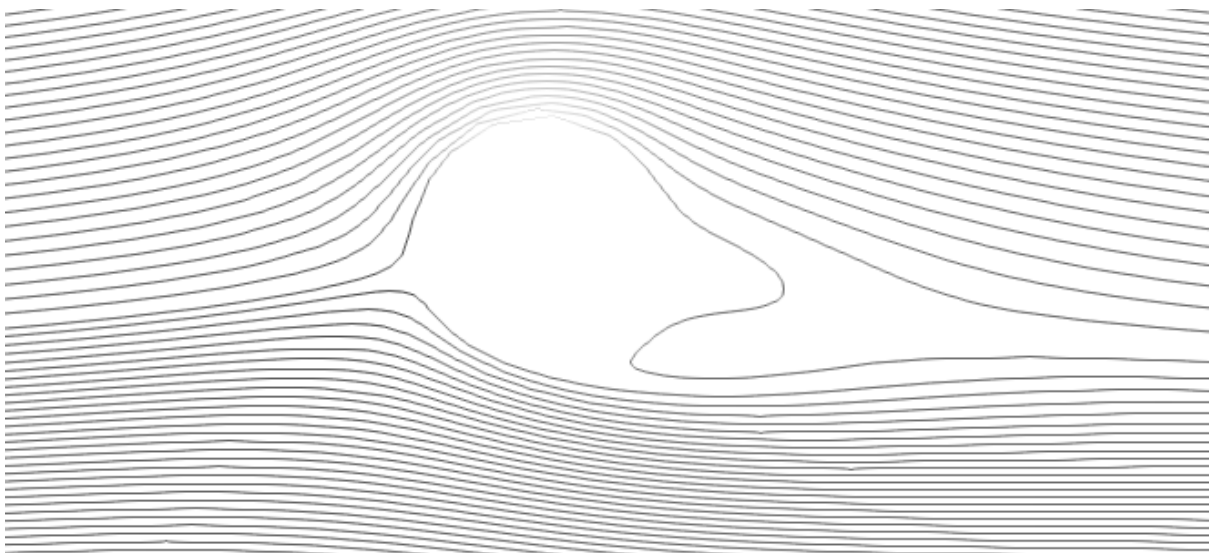The streamlines near the cylinder at $T = 1$ is shown in fig. 9

Figure 9. Streamlines at $T = 1$ near the cylinder.

The streamlines at $T = 1$, as shown in fig. 9, agree well with literature [2]. The two points, where the streamlines are normal to the surface of the cylinder, indicate the two stagnation points. The stagnation point behind is not as well defined as in the front of the cylinder because of turbulence and the formation of vortices in the region.

4.1. Laminar Flow

The problem is simulated for a laminar flow by considering a less viscous fluid with a kinematic viscosity of $\nu = 10^{-2}$ m²/s. The Reynolds number of the flow is $Re = 200$ which is in the laminar regime. The turbulence model is set to laminar. All the other parameters are unaltered.

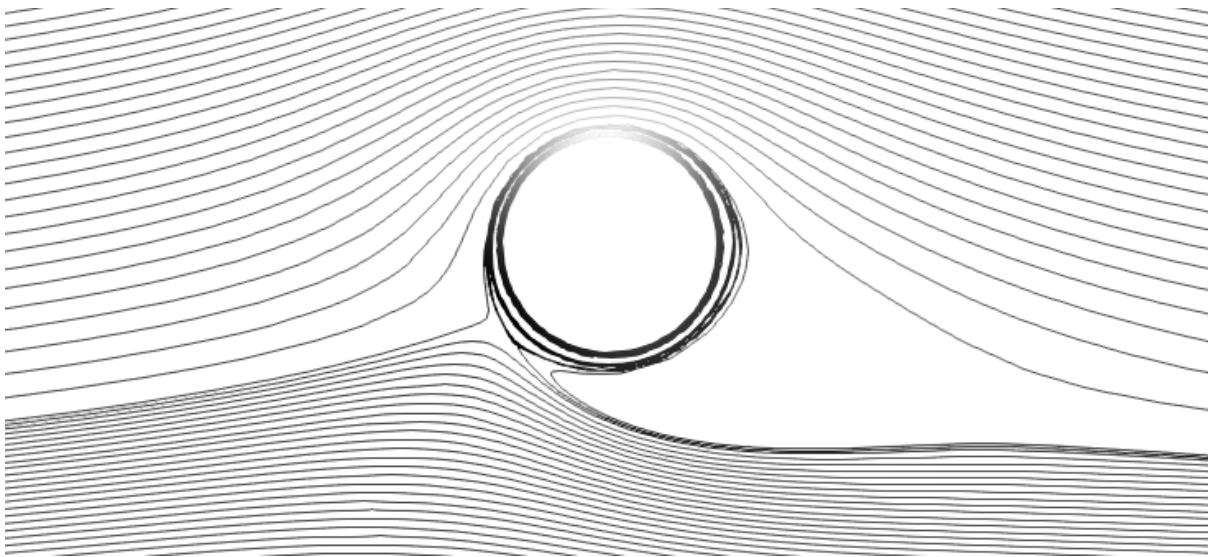The streamlines at $T = 1$ is shown in fig. 10.

Figure 10. Streamlines at $T = 1$ near the cylinder.

On comparison with the streamlines for the turbulent flow (fig. 9), it can be observed that the flow separates much ahead in laminar flow compared to that in turbulent flow. This observation agrees with the literature, with the higher momentum in the boundary layer for the turbulent flow accounting for the same.

5. Conclusion

The turbulent flow across a rotating cylinder was simulated using OpenFOAM solver pimpleFoam. The simulation produced expected result. The phenomenon of Magnus effect was observed. The simulation indicated the presence of pressure difference above and below the cylinder and hence an upward force, known as the Magnus force, on the cylinder. The streamlines agree well with the literature [2] and indicates the presence of vortices behind the cylinder, which is expected in a turbulent flow. The flow was also simulated for a less viscous fluid to study the effects of laminar flow across a rotating cylinder. The delayed flow separation in turbulent flow was observed on comparison with the laminar streamlines for the same flow parameters.

References

1. Anderson, John D. Fundamentals of Aerodynamics. Boston: McGraw-Hill, 2001.

2. Prandtl, L., and O. G. Tietjens: Applied Hydro- and Aeromechanics, United Engineering Trustees, Inc., 1934; also, Dover Publications, Inc., New York, 1957.

3. Nobari, M., & Ghazanfarian, J. (2009). A numerical investigation of fluid flow over a rotating cylinder with cross flow oscillation. *Computers & Fluids*, *38*(10), 2026–2036. doi: 10.1016/j.compfluid.2009.06.008